Advances on the semi-transparent modules based on micro solar cells: First integration in a greenhouse system

Article *in* Applied Energy · January 2016

DOI: 10.1016/j.apenergy.2015.11.002

CITATIONS
38

READS
533

7 authors, including:

Marco Cossu
Università degli Studi di Sassari
25 PUBLICATIONS **260** CITATIONS
SEE PROFILE

Zhi Li
Chinese Academy of Sciences
7 PUBLICATIONS **64** CITATIONS
SEE PROFILE

Josuke Nakata
19 PUBLICATIONS **208** CITATIONS
SEE PROFILE

Applied Energy 162 (2016) 1042–1051

Contents lists available at ScienceDirect

Applied Energy

journal homepage: www.elsevier.com/locate/apenergy

Advances on the semi-transparent modules based on micro solar cells: First integration in a greenhouse system

Marco Cossu [a], Akira Yano [a,*], Zhi Li [a], Mahiro Onoe [a], Hidetoshi Nakamura [b], Toshinori Matsumoto [b], Josuke Nakata [c]

[a] Faculty of Life and Environmental Science, Shimane University, 1060 Nishikawatsu, Matsue, Shimane 690-8504, Japan
[b] Sphelar Power Corporation, 2F Karasuma-Nijo bldg. 267 Makieya-cho Nakagyo-ku, Kyoto 604-0857, Japan
[c] Kyosemi Corporation, 949-2 Ebisu-cho Fushimi-ku, Kyoto 612-8201, Japan

HIGHLIGHTS

- A semi-transparent photovoltaic module was developed for greenhouse applications.
- Spherical micro-cells with 1.2 mm diameter were embedded in the module.
- The module size matches the roof panel and the sunlight eclipsing level was 9.7%.
- The module conversion efficiency was 0.2% over wide incident angles of sunlight.
- The semi-transparent module allows the co-production of crops and energy.

GRAPHICAL ABSTRACT

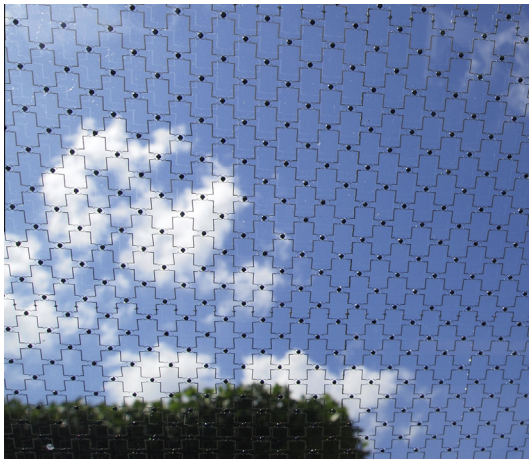

ARTICLE INFO

Article history:
Received 24 April 2015
Received in revised form 30 September 2015
Accepted 4 November 2015

Keywords:
Sunlight
Shading
Renewable energy
Sustainability
Crop

ABSTRACT

The spherical micro-cells are a semi-transparent photovoltaic (PV) technology which can contribute to improve the sustainability of greenhouse systems. Previous prototypes were tested in laboratory conditions, but the size was not suitable for the greenhouse roof application. In this work, a new prototype has been developed and tested on a real greenhouse roof. The semi-transparent PV module (STM) was composed by 4800 spherical silicon micro-cells (1.2 mm diameter) sandwiched between glass plates and integrated on a greenhouse roof with 26.5° slope. The STM was 910 mm long and 610 mm wide to match the size of the greenhouse framework. The percentage of the STM area covered with micro-cells was 2.3%, reaching 9.7% considering the metallic conductors. The cell density was 2 cells cm^{-2} and the measured perpendicular light transmissivity of the semi-transparent area was 73%. The characteristics of the prototype were compared with those of a conventional planar multi-crystalline silicon module (CPM). The module conversion efficiency was steadily around 0.2% over wide incident sunlight angle. The micro-cells never completely eclipse the incident sunlight when observed from more than 1 m distance from

* Corresponding author. Tel./fax: +81 852 32 6543.
E-mail address: yano@life.shimane-u.ac.jp (A. Yano).

http://dx.doi.org/10.1016/j.apenergy.2015.11.002
0306-2619/

the roof, keeping the eclipsing level at 9.7%. The yield factor of the STM was slightly higher than the CPM because of the isotropic properties of the spherical cells, which are able to use both the sky-incident and the ground-reflected irradiation for energy production, irrespective of the module slope. The prototype STM is promising for greenhouse roof applications and its performance can be improved by increasing the conversion efficiency.

1. Introduction

A greenhouse improves the yield and quality of crop productions by means of micro-climate optimisation. The environment control in greenhouse systems is an energy-demanding technique affecting the profit and loss of greenhouse crop production [1–3]. The economic competitiveness of the greenhouse depends also on the capability of saving and self-producing energy to partly or completely cover the demand. Photovoltaic (PV) energy is the most popular renewable source in Europe [4, 5], already examined in the greenhouse sector for powering various climate control applications [6–10]. The same area on which the greenhouse is located can be partly used for installing PV systems, thereby producing energy without consuming additional land for agricultural activities or restricted by regulations. Accordingly, the PV greenhouse integrates a PV array on the roof, with the attempt of finding the best compromise between energy and food production on the same area, thus optimising the integrated system [11, 12].

The solar radiation available inside a PV greenhouse decreases with the ratio of the roof area covered with panels and it is distributed with a high variability over the greenhouse area, depending on the sun position, the portion of the area considered, and the roof panel configurations [13]. The yield is strictly related to the light availability [14–16], decreasing by nearly 1% for every 1% reduction of solar radiation for a large variety of greenhouse crops including vegetables and flowers [17]. As a consequence, the irregular distribution of the solar radiation in a PV greenhouse affects crop growth and productivity differently depending on the position of the plants on the cultivation area. The uniformity of the light distribution can be improved by increasing the gutter height, installing the PV array on both roofs, or arranging the PV panels using a checkerboard pattern [18–20].

The crop response is essentially related to the species considered and the characteristics of the PV greenhouse. Yield reduction of tomato was not observed inside a greenhouse with a 9.8% PV coverage, despite negative effects observed on the fruit size and colour [21]. A crop yield loss of 25% was observed for Welsh onion, when the PV coverage was 13% [22]. The biomass production and yield of basil and zucchini were not affected significantly by a PV coverage of around 20% [23]. Most PV greenhouses in southern Europe have been realised with the specific purpose of maximising energy production. The structures have often been built following an east–west orientation, with the entire south-oriented roofs (50% of the total roof area) covered with conventional planar multi-crystalline silicon panels and roof slopes around 22° [24]. In this case, the solar radiation is distributed following a north–south gradient at the canopy level. The greenhouse areas under the PV roof receive 82% less solar energy than a conventional greenhouse without PV array, whereas the reduction under the plastic cover is 46%, on average.

The semi-transparent PV technology is considered a good compromise between electrical production and light transmissivity in greenhouse systems because they usually shade only a fraction of the incident solar radiation and can maintain the uniformity of light distribution over the greenhouse area. The products based on multi-crystalline or amorphous silicon have already been tested and applied on residential, commercial and office buildings [25–27]. They can be based on conventional planar silicon PV cells, flexible thin films, CIS or CIGS semiconductors [18, 28–30].

Other semi-transparent panels are based on spherical silicon micro-cells, as described already by Yano et al. [31]. The first prototype was based on spherical cells with 1.8 mm diameter with a sunlight eclipsing percentage of 39%. The solar radiation would be distributed homogeneously over the greenhouse area because the dimension of the small cells was not enough to completely eclipse the sun observed from plants. This feature can be distinguished from the semi-transparency of PV modules based on conventional cells, where the sun is completely eclipsed. Furthermore, they can use the sun-rays coming from any spatial direction, thereby producing a constant amount of energy over a wide range of sunlight incident angles. The prototype demonstrated the advantage of the spherical micro-cells, but the module still needed to be tested on the field and it was too small (97 cm^2) and thick (11 mm) for greenhouse roof applications.

In this study, a new prototype of semi-transparent module (STM) covered with spherical micro-cells and conductors was designed. The sunlight eclipsing percentage was calibrated referring to the light requirements of tomato, which is considered the most light-demanding greenhouse crop [32, 33]. As a reference concerning tomato cultivation inside PV greenhouses, Ureña-Sánchez et al. [21] reported no yield loss when the PV cover was 9.8% of the greenhouse roof area. Therefore, the new STM prototype has been designed with a similar sunlight eclipsing percentage of 9.7%, thus providing a transparency about four times potentially higher than the previous prototype. The module size was compatible with the dimensions of common greenhouse glass panels. Therefore, it has been integrated and tested on the roof of a real greenhouse. The shading of the PV panel over the greenhouse area has been measured and the electrical performance of the prototype has been compared with that of a conventional planar multi-crystalline silicon module (CPM).

2. Materials and methods

2.1. Spherical solar micro-cells and the semi-transparent PV module

Mono-crystalline silicon spherical PV cells of 1.2 mm diameter (Sphelar®; Sphelar Power Corp., Kyoto, Japan) were used (Fig. 1a). The PV cells were composed of a *p*-type semiconductor as the inner core and an *n*-type semiconductor as the outer shell [34, 35]. The power output is drawn through electrodes.

The STM was assembled using 4800 cells with a density of 2 cells cm^{-2} (Fig. 1b and c). The module was 910 mm × 610 mm to match the size of the greenhouse roof framework size. The cells were distributed across a 501 mm × 480 mm area, of which 2.3% was covered with the cross-sectional area of the cells and 7.4% with 0.3 mm wide metallic conductors, connecting the cells to feed current to the output terminals of the module. The 4800 cells were sandwiched between 3-mm-thick glass plates after they were embedded in 2-mm-thick transparent resin. Thereby, the STM was optically bifacial. The thickness of the module was 8 mm

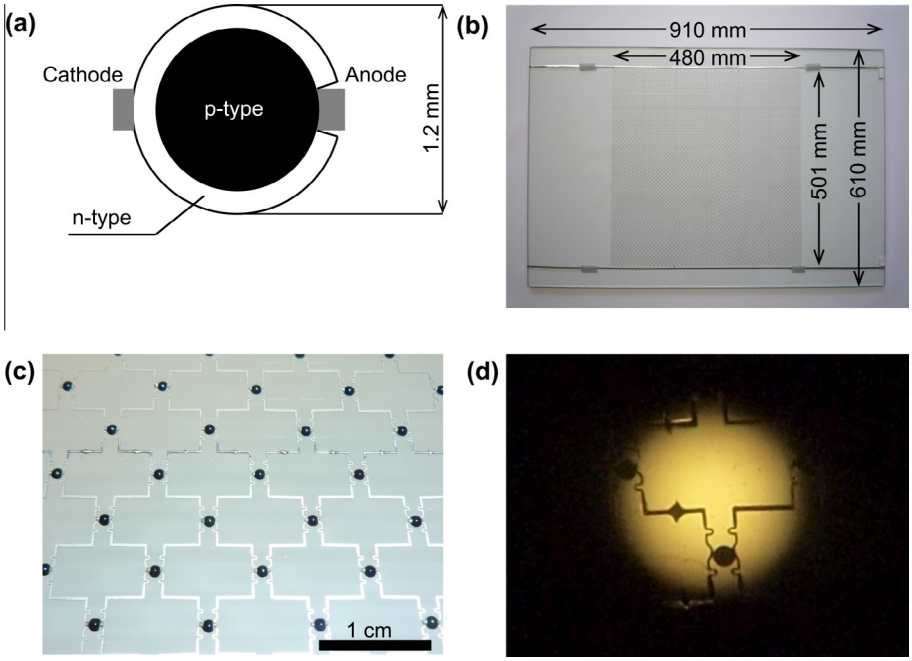

Fig. 1. Cross-sectional view of the structure of the spherical solar micro-cell (Sphelar®, a) and the prototype of the semi-transparent PV module (b) with 2 cells cm^{-2} density (c). A photograph (d) showing overlapping of the PV cells over the sun was taken from 1.0 m below the module through a solar-eclipse observation filter mounted on a digital camera lens.

and the weight was 4 kg. In the STM, 50 cells with 10 mm mutual separation were aligned so that every anode of the 50 cells was soldered directly to a conductor and every cathode was soldered to another conductor (Fig. 1c). The small curves of the zig-zag shape conductors were designed to absorb shrinkage and extensions of the cell alignment during the thermal process of resin solidification. The 50 cells were connected electrically in parallel. By repeating this process, 32 pairs of the 50 parallel cells were connected electrically in series. Finally, three pairs of the 32 series connections were connected in parallel. The rated power output of the STM was 463 mW, the optimum operating voltage is 12.87 V, and the optimum operating current is 36.0 mA for the Standard Test Conditions (STC: 1 kW m^{-2} single side irradiation, 25 °C cell temperature) with air mass of 1.5, which is a typical solar spectrum on the earth's surface on a clear day [36].

Fig. 1d portrays the overlapping of the PV cells over the sun. The picture was taken at 1.0 m below the module through a solar eclipsing observation filter mounted on a digital camera lens. From an observation point of 0.13 m below the module, the cross-sectional area of the sun projected on the STM coincides with the cross-sectional area of a single spherical PV cell, resulting in perfect shading of the direct sun beam. As the distance between the module and the observation point increases, the eclipsing percentage by the cells and the conductor wires converges to 9.7%, corresponding to the percentage of the cross sectional area of the cells and the conductors of the 501 mm × 480 mm module area (see details by Yano et al. [31]). Assuming the use of the STM as a greenhouse roof, the plants are presumed to lie at least 1 m far from the PV modules, thus receiving the minimum and constant eclipsing level (9.7%). Thereby, the direct sunlight cannot be eclipsed completely by the cells when observed from the greenhouse plants. This semi-transparency to the direct solar irradiance onto plants is due specifically to the micro solar cells. Current PV greenhouses use CPMs, which completely shade the direct radiation, causing immoderate reduction of solar irradiation available for the greenhouse crop. The high variability of the sunlight distribution on the greenhouse area can be overcome using the micro-cells. The sky-diffused irradiance reaching the greenhouse depends on the ratio of the cross-sectional areas of both micro-cells and conductors to the entire greenhouse cover area. Accordingly, if the roof and the walls of the greenhouse were made entirely with STMs, 9.7% of global irradiance would be shaded, under the assumption of perfect light transmittance of the module matrix glass and resin.

In the present study, a multi-crystalline CPM (KD03, Kyocera Corp., Kyoto, Japan) was also used for comparison of the electric characteristics to the STM. The dimensions of the CPM were 240 mm × 160 mm with 17 mm thickness including the frame structure. The PV cells in the CPM were arranged in 215 mm × 125 mm area with 4 mm thickness, including the cover glass and an opaque substrate. The rated power output was 3.01 W, the optimum operating voltage was 17.6 V, the optimum operating current was 171 mA and the efficiency was 11.2%, according to the STC.

2.2. Measurements of electrical and shading characteristics of the PV modules

The electrical and shading characteristics of the PV modules were measured in an empty greenhouse (Fig. 2) on the Shimane University campus (35°29′N, 133°04′E) during several partly cloudy days in May, June and October 2014. No cover material, other than the PV modules, was installed on the greenhouse roof. The eastern block of the greenhouse floor was covered with weeds and the remaining area with concrete. Trees beside the east side of the greenhouse did not shade the PV modules during the experiments. The STM was attached to the greenhouse roof frame 3 m above ground. The PV module was inclined 26.5°, according to the greenhouse roof slope. The azimuth of the PV-module's sky-directing normal pointed 6° southerly from the west (Fig. 2a). The current (I)–voltage (V) characteristics of the STM were measured at 1 min intervals, from 9:47 to 16:59 on May 13, and from 8:30 to 16:00 on October 8, using a voltage/current sourcemeter (6241A; ADC Corp., Tokyo, Japan). Pyranometer P_1 (MS-402; Eko Instruments Co. Ltd., Tokyo, Japan) was positioned horizontally

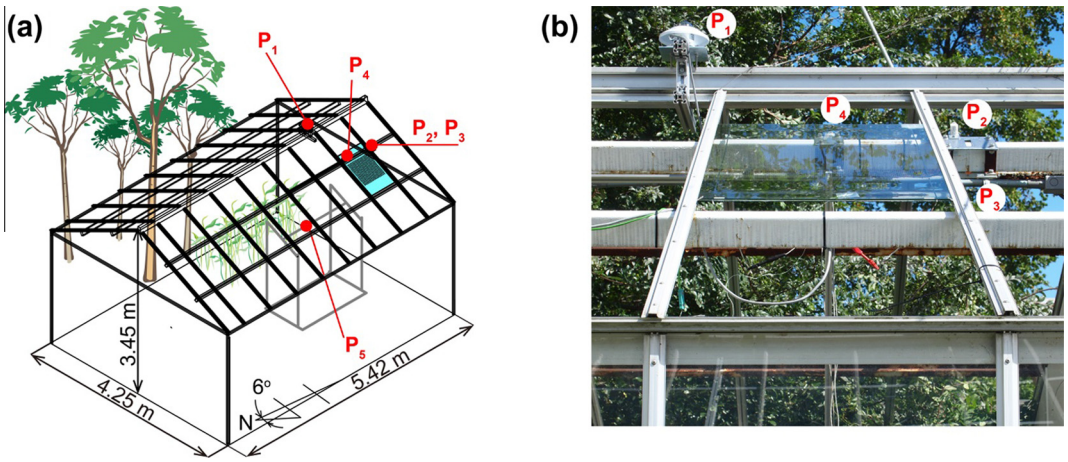

Fig. 2. Configuration of sunlight and shading measurements. The semi-transparent PV module (shown as a pale blue plate) and pyranometers P_1, P_2, P_3, and P_4 were mounted on the greenhouse roof frames (a). P_5 tracked the shadow of the module cell area. P_3 was hidden by the greenhouse framework in the photograph (b), but it was positioned 180° to the opposite side of P_2, directed downward. P_4 was positioned behind the PV module at the margin of the PV cell area.

on the roof top to measure the horizontal global irradiance I_{HT} at 1 min intervals. The global irradiance on the inclined PV-module's top surface I_T and the ground-reflected irradiance on the inclined PV-module's bottom surface $I_{T\rho}$ were measured at 1 min intervals, respectively using pyranometers P_2 and P_3 (ML-020VM; Eko Instruments Co. Ltd.), which were positioned on the top and the bottom of the 26.5° inclined roof beam (Fig. 2). Pyranometer P_4 was positioned immediately behind the margin of the semi-transparent PV cell area to measure the transmissivity of the module's transparent matrix materials made with the layers of glass and resin. The shadow of the 501 mm × 480 mm semi-transparent cell area was tracked manually using the pyranometer P_5 (ML-020VM) positioned on a 26.5° inclined movable bar placed 1 m below the PV module (Fig. 2a). A *K*-type thermocouple (RS 409–4908; RS Components K.K, Yokohama, Japan) was adhered to the bottom face of the PV module margin. The electrical characteristics, irradiance, and module temperature data were transmitted through a GPIB interface and stored synchronously in a computer. The STM was replaced with the CPM (KD03) on June 24 and October 17. The *I*–*V* characteristics of the CPM and irradiance were also measured.

Even though CPM did not use $I_{T\rho}$ for electricity production due to its opaque back cover, it actually received also this fraction of the irradiance. For this reason, to compare the two technologies under the same irradiance conditions, the module efficiency η was defined as the percentage of the maximum power output P_{max} of the PV modules to the impinging irradiance $I_T + I_{T\rho}$ on the 501 mm × 480 mm semi-transparent cell area, or the 215 mm × 125 mm cell area of the CPM. The theoretical values of γ, defined as the angle between direct beam sunlight and the PV-module's upper normal, was calculated at 1 min intervals for the experimental date and site. The irradiance and the electricity production were also calculated theoretically following equations proposed by Yano et al. [37].

3. Results and discussion

During the experiments, the sky condition was partly cloudy. The measured global irradiance on the horizontal plane I_{HT} is depicted in Fig. 3 for each date. The peak I_{HT} values were around 1000 W m^{-2} in May and June. They were around 800 W m^{-2} in October as peak values. We calculated the theoretical I_{HT}s changing the atmospheric transmissivity values stepwise 0.1. Then we chose the best fit theoretical curve closest to the measured I_{HT} curve during the cloudless hours. The calculation approximated the measured I_{HT} curves when the atmospheric transmissivity was assumed as 0.65 in May, 0.68 in June, and 0.80 in October (Fig. 3). The atmospheric transmissivity is usually low in spring and high in autumn in the Shimane area.

Fig. 4 shows the global irradiance on the 26.5° inclined PV-module's top surface I_T, the ground-reflected irradiance on the inclined PV-module's bottom surface $I_{T\rho}$, and the ratio between $I_{T\rho}$ and I_T. The theoretical curves for I_Ts were also shown using the same atmospheric transmissivity values as I_{HT} calculations. The I_T values of the western-sky facing PV modules reached the peak in the afternoon. During October experiments, the ratio $I_{T\rho}/I_T$ was around 10% at midday and higher in the early morning because $I_{T\rho}$ irradiated on the back cover of the PV module from the eastern ground, whereas the direct sunlight from the east sky passed through the upper surface of the western-sky facing PV module. Although $I_{T\rho}$ is not used by the CPM, $I_{T\rho}$ can contribute effectively to the electricity production of the STM. Around midday, the $I_{T\rho}$ contributed about 9% ($=I_{T\rho} \times 100\%/(I_T + I_{T\rho})$) of the electricity production of the STM module.

A distinct pulse in $I_{T\rho}/I_T$ can be observed from 10:57 to 11:06 on October 8 because of an electric transmission line positioned above the greenhouse, which shaded the direct sunlight on pyranometer P_2 during the time period. As a result, only I_T decreased sharply, resulting in a peak in the ratio $I_{T\rho}/I_T$.

Fig. 5 depicts the *I*–*V* and the power output P_{PV}–*V* characteristics of the STM measured at 1 min intervals. I_T peaked at 13 h for the west-facing PV module, causing the *I* and P_{PV} peaks during that time period. The peak currents of the STM exceeded 40 mA. Correspondingly, the peak power approached 0.5 W. The CPM generated more than 200 mA and 3 W on June 24 (Fig. 6). The maximum peak value (P_{max}) of the STM's P_{PV}–*V* curve was 0.500 W at 13:00 on October 8. At that moment, $I_T + I_{T\rho}$ was 1057 W m^{-2}, the open circuit voltage was 16.03 V, the short circuit current was 46.13 mA, the optimum operating voltage was 12.39 V, the optimum operating current was 40.32 mA, and the fill factor was 0.68, where the product of the optimum operating voltage and current provides P_{max}. The fill factor is defined as the ratio of P_{max} to the product of the open circuit voltage and the short circuit current [36]. A higher fill factor corresponds to higher efficiency. The maximum P_{max} value of the CPM was 3.109 W at 12:53 on June 24. At that moment, $I_T + I_{T\rho}$ was 1257 W m^{-2}, the open circuit voltage was 20.64 V, the short circuit current was 220.9 mA, the optimum operating voltage was 16.27 V, the optimum operating current was 191.1 mA, and the fill factor was 0.68.

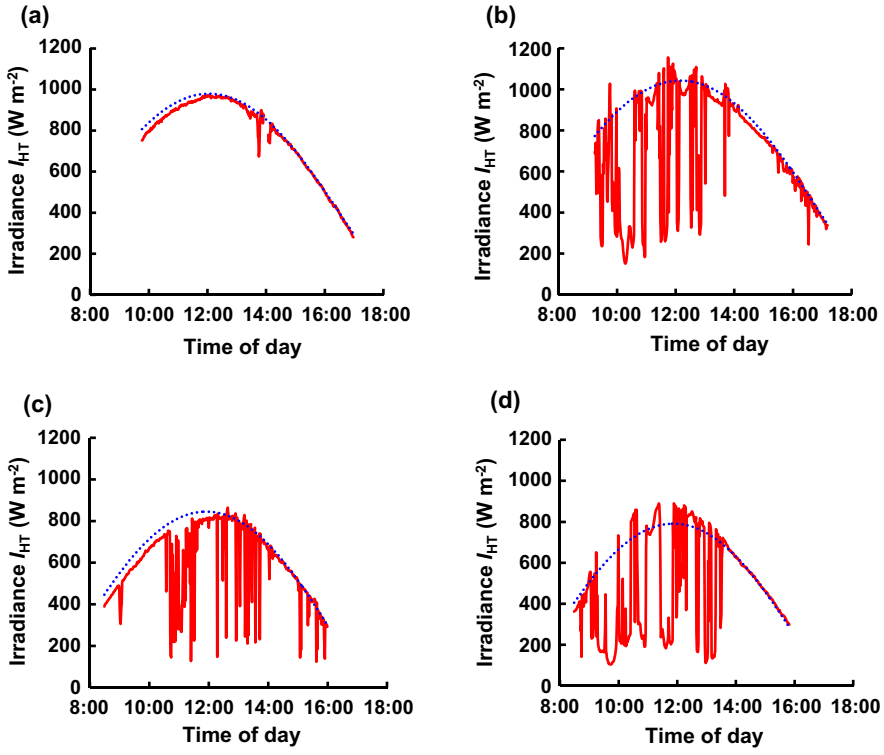

Fig. 3. Measured (red lines) and calculated (dotted blue lines) global irradiance on the horizontal plane I_{HT} on May 13 (a), June 24 (b), October 8 (c), and October 17 (d). Atmospheric transmissivities p = 0.65, 0.68, and 0.8 were used respectively for May, June, and October calculations. (For interpretation of the references to colour in this figure legend, the reader is referred to the web version of this article.)

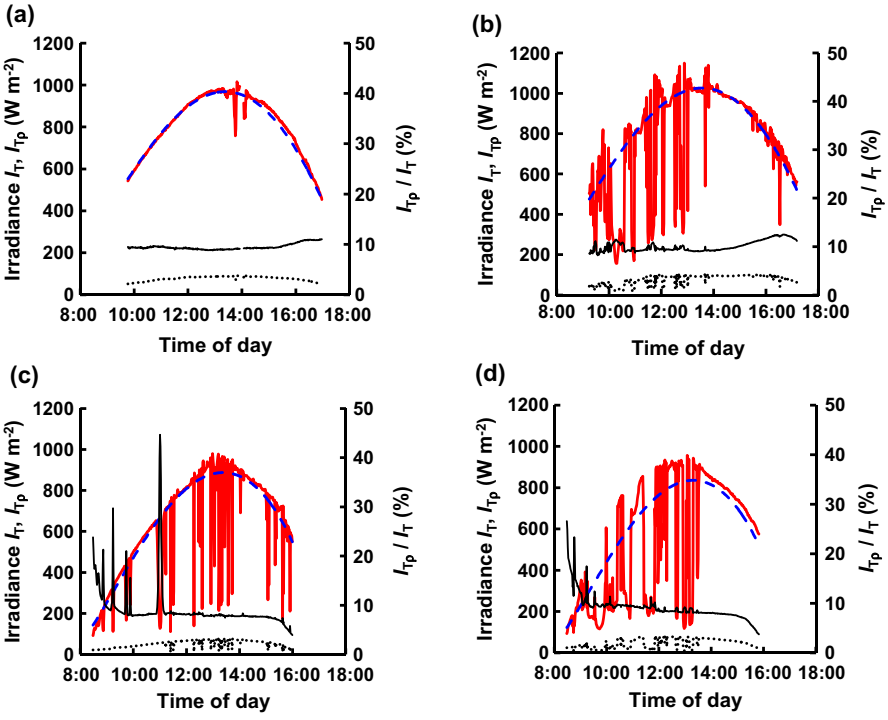

Fig. 4. Measured (bold-solid red lines) and calculated (dashed blue lines) global irradiances I_T on the western-sky facing and 26.5° inclined PV-modules' top-surfaces, ground-reflected irradiances $I_{T\rho}$ on the PV-modules' bottom surfaces (dotted black lines), and the $I_{T\rho}/I_T$ percentage (solid black lines) on May 13 (a), June 24, (b), October 8 (c), and October 17 (d). (For interpretation of the references to colour in this figure legend, the reader is referred to the web version of this article.)

Fig. 7 shows the relation between $I_T + I_{T\rho}$ and the normalised P_{max} (W m^{-2}), which is derived by dividing P_{max} with the 501 mm × 480 mm semi-transparent cell area of the STM or the 215 mm × 125 mm cell area of the CPM. Irrespective of the experimental season, the normalised P_{max} increased linearly with the increase of $I_T + I_{T\rho}$. The normalised P_{max} values of the CPM were about 50 times higher than those of STM through the whole $I_T + I_{T\rho}$ range. The efficiency values η of the STM and CPM were

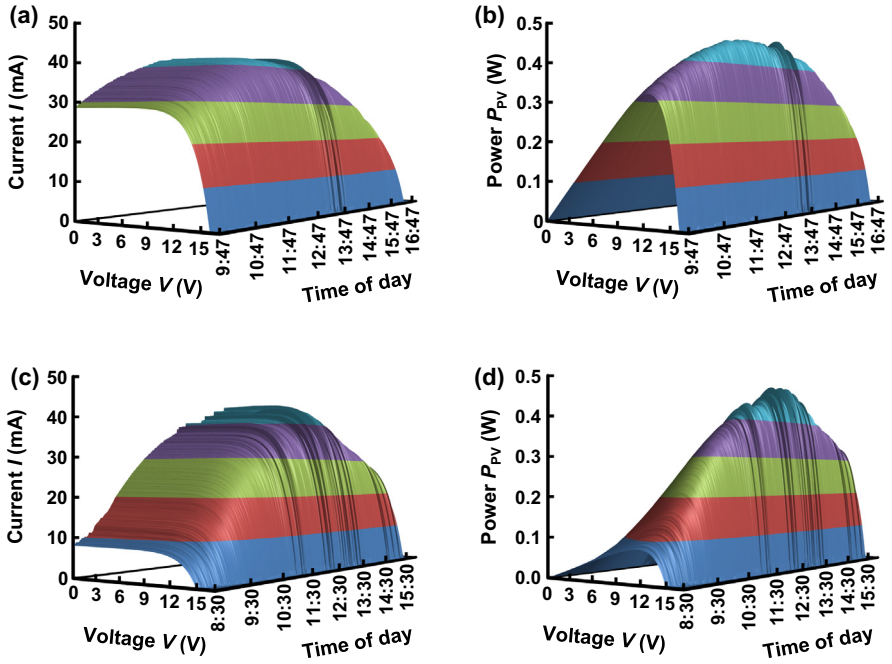

Fig. 5. *I–V* (a and c) and P_{PV}–*V* (b and d) characteristics of the semi-transparent PV module measured on May 13 (a and b) and on October 8 (c and d).

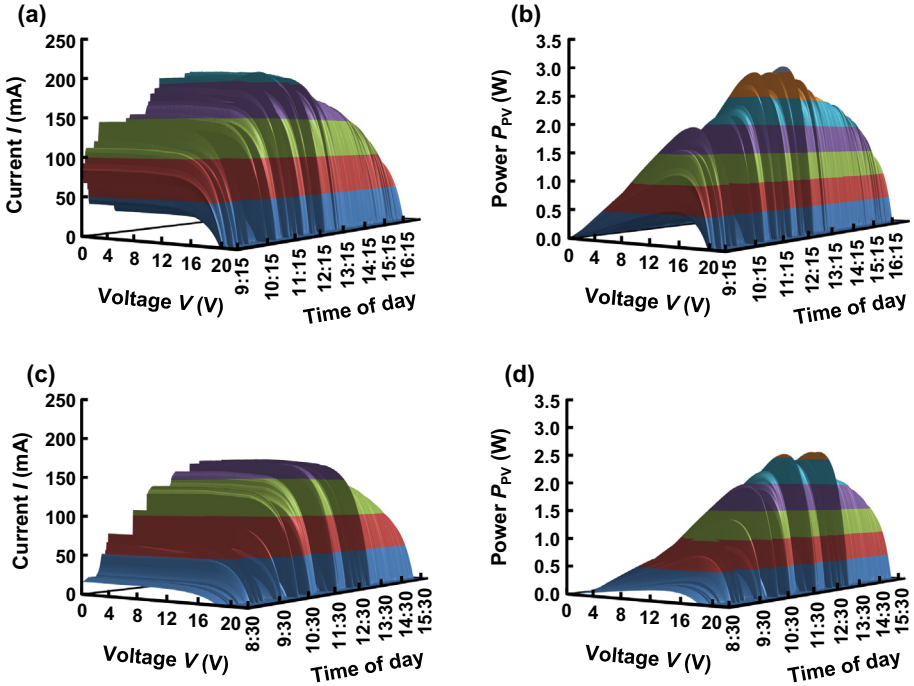

Fig. 6. *I–V* (a and c) and P_{PV}–*V* (b and d) characteristics of the conventional planar PV module measured on June 24 (a and b) and on October 17 (c and d).

respectively 0.2% and 9% (Fig. 7c and d). The distinct increase of η can be attributed to pyranometer P_2 shading between 10:57 and 11:06 on the October 8 experiment, as described in the Materials and methods section.

Fig. 8a depicts the calculated angle γ between the direct sunlight incidence and the sky-directing PV-module's normal during each experiment. The γ values were 10.5–86.2° for the STM and 5.7–87.4° for the CPM. The normalised P_{max} decreased as γ increased (Fig. 8c and d) and taking dual values for a single γ, for example around $\gamma = 30°$, as shown in the open red circles in Fig. 8c. This result was due to the PV module, receiving direct sunlight from the equivalent γ angles twice before and after 14 h (Fig. 8a), while global irradiance was lower after 14 h. Consequently, the normalised P_{max} values after 14 h were lower than those before 14 h for the same γ value. The module efficiencies η were consistently around an average of 0.2% for the STM and 9% for the CPM over a wide γ range. The constant η of the STM can be attributed to the isotropic photoreception of the spherical cells, the bifacial transparency of the module and the module temperature drop in the high γ range (Fig. 9). The CPM temperature was

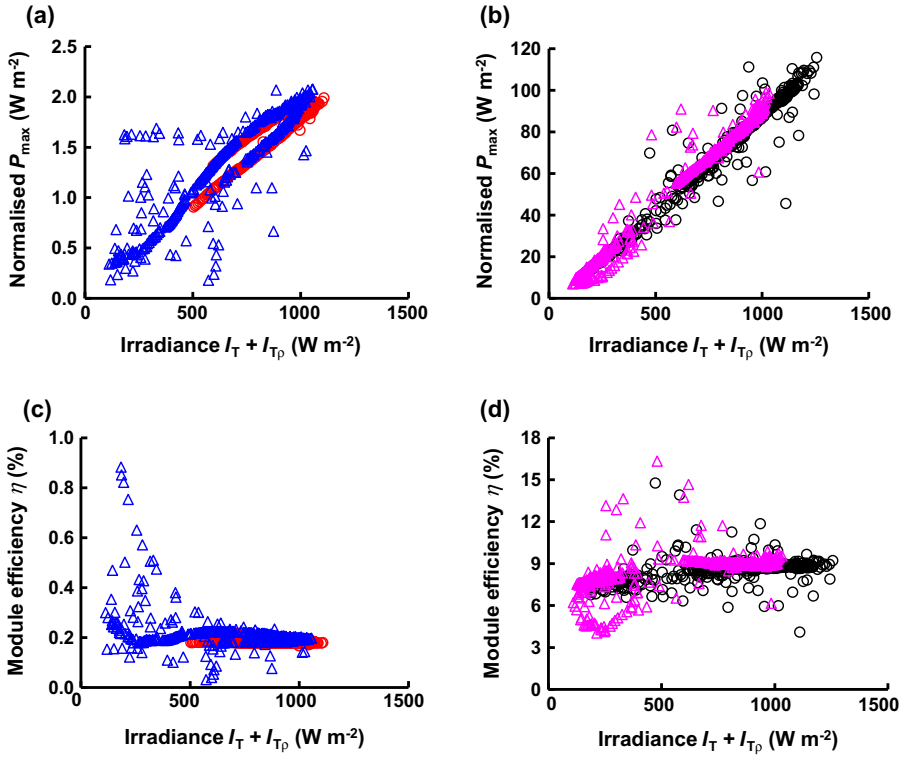

Fig. 7. Relation between normalised peak PV power output P_{max} and $I_T + I_{T\rho}$ of the STM (a) on May 13 (open red circles) and October 8 (open blue triangles) and those of the CPM (b) on June 24 (open black circles) and October 17 (open pink triangles), and the relation between module efficiency η and $I_T + I_{T\rho}$ of the STM (c) on May 13 (open red circles) and October 8 (open blue triangles) and those of the CPM (d) on June 24 (open black circles) and October 17 (open pink triangles). (For interpretation of the references to colour in this figure legend, the reader is referred to the web version of this article.)

higher than that of STM in the low γ range because the CPM was thinner. Consequently, the heat of the PV surface was transferred easily to the backside of the module, where the thermocouple was attached. The contribution of $I_{T\rho}$ for electricity production increased in the morning for the STM and maintained η constant during the high γ hours. However, $I_{T\rho}$ did not contribute to electricity production of the CPM, resulting in a η drop in the high γ range because $I_{T\rho}$ was in the denominator of the efficiency equation.

The annual electrical energy produced per unit of greenhouse ground area was calculated for an A-Frame greenhouse with 26.5° roof slope, using STM (η = 0.2% with dual-side irradiation) or the CPM (η = 11.2% with single-side irradiation), which can be installed on the entire roof or on the half side roof, assuming a clear sky condition (Table 1). The PV roof would produce 5.5 kW h m^{-2} yr^{-1} ground area if the STM covered the entire roof of an east–west oriented greenhouse. The PV roof would produce 2.1 kW h m^{-2} yr^{-1} if only the north roof were covered with the STM. For an STM covering the entire roof of a north–south oriented greenhouse, the PV roof would produce 5.6 kW h m^{-2} yr^{-1}. This value is comparable to that of the STM covering the entire roof of the east–west oriented greenhouse. The CPM produced 50 times more energy (kW h m^{-2} yr^{-1}) than the STM. The annual electrical energy consumption per unit greenhouse ground area of various greenhouse locations and electrical loads was reported from 2 to 20 kW h m^{-2} yr^{-1} among Mediterranean greenhouses [31]. The electricity production of the STM can therefore be considered marginal or insufficient, even for greenhouses located in highly-irradiated regions, where higher yield factors are expected.

The yield factor is the net AC energy output of the PV system (kWh) divided by the peak power of the installed PV array (kWp) at standard test conditions (STC: irradiance 1000 W m^{-2} and 25 °C cell temperature) [39]. The annual yield factor of the STM is slightly higher than the CPM, due to the use of the ground-reflected radiation (Table 2). Estimations have been conducted using the electricity production data from the PVGIS web software [38]. In southern European countries, where PV greenhouses are widely spread, the annual energy production per unit of STM area is 1.9–3.1 kW h m^{-2}, according to the roof orientation. The yield factor can reach up to 1750 kW h kWp^{-1} when the STMs are south-oriented, compared to the 1590 kWh kWp^{-1} of PV systems with CPMs. However, a PV array area of 472 m^2 kWp^{-1} is required by the STM, compared to the CPM (8.9 m^2 kWp^{-1}), rendering the conventional technologies still preferable for high PV power installations.

In the afternoon of May 13, the shadow of STM cell area was tracked by pyranometer P_5, placed 1 m below the PV module (Fig. 2). Pyranometer P_4 measured the transmissivity of the STM matrix during the same time period. Fig. 10 presents the measured transmissivities of the STM matrix structure and the STM cell area. The mean perpendicular light transmissivities of the matrix structure and the STM cell area were, respectively, 82% and 73%. Therefore, only 73% of the sunlight impinging on an STM greenhouse roof can be used for plant cultivation. The remaining part (27%) should consider the cross-sectional area of the 4800 cells of the STM (2.3%), with an assumed conversion efficiency of 10%. In this case, the cross-sectional area of the cells can use 0.23% of the sunlight for electricity production (2.3% × 0.10). As a consequence, 26.8% (27–0.23%) of the sunlight was not used either for plant growth, or for electricity production.

On the other hand, if a greenhouse roof is entirely covered with CPMs, then 0% of sunlight impinged on the opaque CPM greenhouse roof can be used for plant cultivation. About 10% of the sunlight (equal to the assumed conversion efficiency) not reaching the greenhouse plants can be converted into electricity. As a

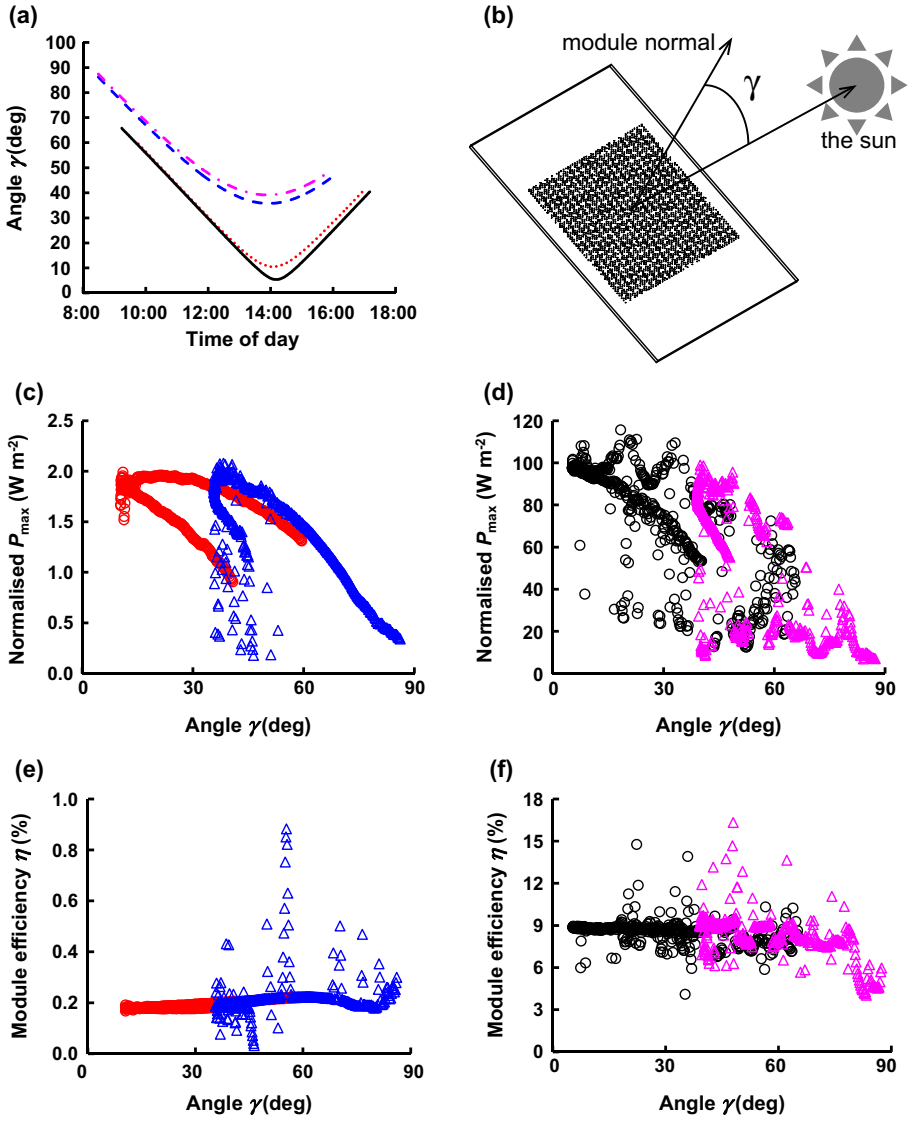

Fig. 8. Calculated angle γ (a, see also b for the definition) of the STM on May 13 (dotted red line) and October 8 (dashed blue line) and of the CPM on June 24 (solid black line) and October 17 (dot-dashed pink line). The relations between normalised P_{max} and γ of the STM (c) on May 13 (open red circles) and October 8 (open blue triangles) and those of the CPM (d) on June 24 (open black circles) and October 17 (open pink triangles) are shown. The relations between η and γ of the STM (e) on May 13 (open red circles) and October 8 (open blue triangles) and those of the CPM (f) on June 24 (open black circles) and October 17 (open pink triangles). (For interpretation of the references to colour in this figure legend, the reader is referred to the web version of this article.)

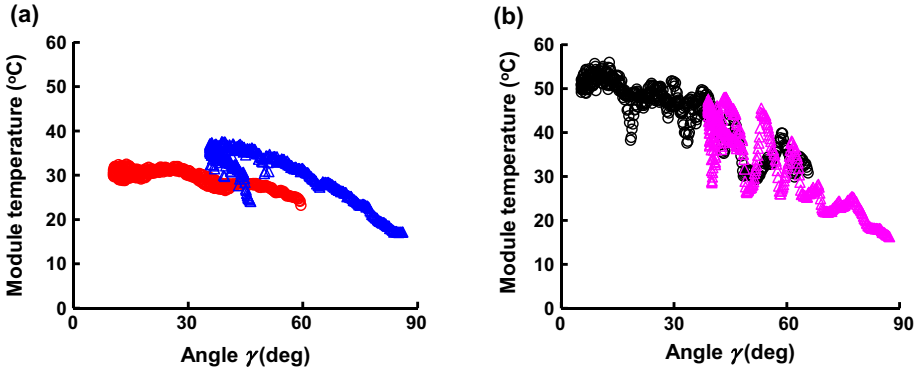

Fig. 9. Relations between module temperature and γ of the STM (a) on May 13 (open red circles) and October 8 (open blue triangles) and those of the CPM (b) on June 24 (open black circles) and October 17 (open pink triangles). (For interpretation of the references to colour in this figure legend, the reader is referred to the web version of this article.)

Table 1
Estimation of annual electrical energy production and peak power developed by the STM and the CPM mounted on a greenhouse roofs.

Greenhouse orientation	PV module	PV roof coverage	Energy per unit of tilted module area* (kW h $m^{-2}yr^{-1}$)	Energy per unit greenhouse area (kW h $m^{-2}yr^{-1}$)	Module peak power per unit module area (kWp m^{-2})	Module peak power per unit greenhouse area (kWp m^{-2})
East–west	STM	South roof only	6.0	3.3	0.0021	0.0012
		North roof only	3.8	2.1	0.0021	0.0012
		South and north roofs	4.9	5.5	0.0021	0.0024
	CPM	South roof only	307.9	172.0	0.1120	0.0626
		North roof only	188.5	105.3	0.1120	0.0626
		South and north roofs	248.2	277.3	0.1120	0.1251
North–south	STM	East or west roof only	5.0	2.8	0.0021	0.0012
		East and west roofs	5.0	5.6	0.0021	0.0024
	CPM	East or west roof only	252.6	141.1	0.1157	0.0646
		East and west roofs	252.6	282.3	0.1157	0.1293

STM rated power = 0.463 W; CPM rated power = 3.01 W; STM area = 0.501 × 0.480 m^2; CPM area = 0.215 × 0.125 m^2.
* Atmospheric transmissivity = 0.80; albedo = 0.10; cloudless sky; module inclination = 26.5°; present study location (35°29′N, 133°04′E).

Table 2
Average annual energy production and yield factor estimation of the STM and CPM on a surface tilted 26.5°, for different orientations in Europe.

Greenhouse orientation	PV module	PV roof coverage	Southern Europe[a]		Central Europe[b]		Northern Europe[c]	
			Energy per unit of module area (kW h m^{-2} yr^{-1})	Yield Factor range (kW h kWp^{-1})	Energy per unit of module area (kW h m^{-2} yr^{-1})	Yield Factor range (kW h kWp^{-1})	Energy per unit of module area (kW h m^{-2} yr^{-1})	Yield Factor range (kW h kWp^{-1})
East–west	STM	South roof only	3.1	1360–1750	2.1	1030–1250	2.0	980–1080
		North roof only	1.9	810–1080	1.3	640–780	1.1	570–600
		South and north roofs	2.5	1090–1410	1.7	840–1010	1.6	780–840
	CPM	South roof only	166	1240–1590	112	940–1140	106	890–980
		North roof only	99	740–980	70	580–700	60	520–550
		South and north roofs	132	990–1280	91	760–920	83	710–770
North–south	STM	East or west roof only	2.6	1120–1430	1.8	860–1040	1.6	790–860
		East and west roofs	2.6	1120–1430	1.8	860–1040	1.6	790–860
	CPM	East or west roof only	136	1020–1300	93	780–940	85	720–780
		East and west roofs	136	1020–1300	93	780–940	85	720–780

The yield factor has been calculated using electricity production data from the PVGIS web software [38], for the following locations in Europe: Estimations were performed using the Climate-SAF PVGIS database assuming the use of crystalline silicon PV technologies, an overall efficiency coefficient of the PV system of 85% and considering the losses deriving from temperature and angular reflectance effects.
[a] Valencia, Madrid, Barcelona, Cagliari, Naples, Rome, Milan, Ragusa, and Athens.
[b] Paris, Lyon, Frankfurt, Munich, Berlin, and Amsterdam.
[c] Copenhagen, Stockholm, Edinburgh.

consequence, 90% of the sunlight incident on the CPMs has no role for either plant growth or electricity production. The CPM requires only 2% of the greenhouse roof to produce the same amount of electricity generated by a roof entirely covered with STMs, because the CPM produces 50 times more electricity than STM (1/50 = 0.02). The clear roof area (98%) can supply the sunlight to the crop with an assumed transmissivity of 80% for greenhouse glass.

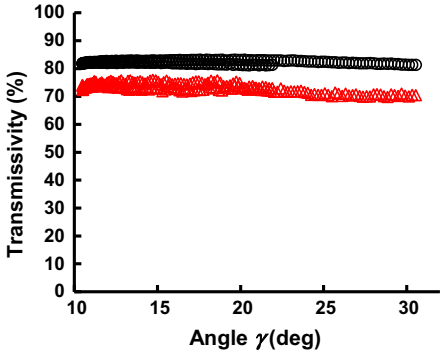

Fig. 10. Measured transmissivity of global irradiation of the transparent module matrix made of the layers of glass and resin (black open circles) and the STM cell area (red open triangles) on May 13. (For interpretation of the references to colour in this figure legend, the reader is referred to the web version of this article.)

Then, the unused fraction of incoming sunlight would be 21.6% (=1–0.98 × 0.8), which decreases to 21.4% (=21.6–2% × 10%), when considering the conversion efficiency.

This aspect suggests that the partial roof coverage with CPM results in a higher sunlight usage in a PV greenhouse crop and electricity co-productions. However, greenhouses are usually shaded with shading screens or painting in summer and high irradiated regions. For this reason, the transparency of the 98% area not covered with CPM would be consistently lower than 80%, and the reflected fraction of light would not be used either by the plants, or by the PV array. On the contrary, the need for shading devices may be avoided or limited by using STM, resulting in an advantage compared to CPM. Diffuse greenhouse glass is also a possible option when only part of greenhouse roof is covered with CPMs [30]. The diffuse glass may mitigate the sharp shading of CPMs and the strong beam irradiance impinged in the greenhouse. Therefore, the balance of the light distribution for plant growth and electricity production should be designed carefully according to the nature of the light requirements of cultivated plants in the greenhouse.

4. Conclusions

The main challenge of PV greenhouses is to produce energy and crops on the same land unit by limiting the shadow casted over the

plants by the PV panels. In this study, the prototype of a STM based on spherical silicon micro-cells has been tested on a greenhouse roof. The diameter of the micro-cells was 1.2 mm. Their cross-sectional area together with opaque conductors covered 9.7% of the module area. The shading produced by the module on the greenhouse area was measured and the electrical performance was compared with a CPM. The conversion efficiency of the STM was stable at around 0.2% and was not affected by the slope angle, because of the isotropic photoreception of the spherical micro-cells. The eclipsing level of the STM was 9.7% and the cell shadow never covers the plants entirely when the distance between the module and the crop is greater than 1 m. This aspect allows a better distribution of the solar radiation on the underlying area, compared to conventional PV panels. Moreover, it makes the semi-transparent spherical micro-cell technology suitable for application to the roof and walls of greenhouses.

The yield ratio of the STM module was slightly higher than those of CPMs because of its capability of using also the ground-reflected radiation for energy production. However, the energy produced by the STM is still insufficient to fulfil the greenhouse electrical demands which are consumed in Mediterranean greenhouses equipped with basic climate control appliances. Further improvements of the technology and manufacturing process are necessary to increase the conversion efficiency and the light transmissivity of the module.

Acknowledgements

The first author, as an International Research Fellow of the Japan Society for the Promotion of Science (JSPS) acknowledges the financial support from JSPS (Grant No. 26•04085). This study was supported by JSPS KAKENHI Grant Numbers 24580370 and 26•04085, and JST A-STEP Grant Number AS262Z00133L.

References

[1] Bot GPA. Developments in indoor sustainable plant production with emphasis on energy saving. Comput Electron Agric 2001;30():151–65. http://dx.doi.org/10.1016/S0168-1699(00)00162-9.
[2] Chen J, Xu F, Tan D, Shen Z, Zhang L, Ai Q. A control method for agricultural greenhouses heating based on computational fluid dynamics and energy prediction model. Appl Energy 2015;141:106–18. http://dx.doi.org/10.1016/j.apenergy.2014.12.026.
[3] Vadiee A, Martin V. Energy analysis and thermoeconomic assessment of the closed greenhouse – the largest commercial solar building. Appl Energy 2013;102:1256–66. http://dx.doi.org/10.1016/j.apenergy.2012.06.051.
[4] Castellano NN, Parra JAG, Valls-Guirado J, Manzano-Agugliaro F. Optimal displacement of photovoltaic array's rows using a novel shading model. Appl Energy 2015;144:1–9. http://dx.doi.org/10.1016/j.apenergy.2015.01.060.
[5] Cruz-Peragón F, Casanova-Peláez PJ, Díaz FA, López-García R, Palomar JM. An approach to evaluate the energy advantage of two axes solar tracking systems in Spain. Appl Energy 2011;88(12):5131–42. http://dx.doi.org/10.1016/j.apenergy.2011.07.018.
[6] Al-Ibrahim A, Al-Abbadi N, Al-Helal I. PV greenhouse system – system description, performance and lesson learned. Acta Hort 2006;710:251–64.
[7] Al-Shamiry FMS, Ahmad D, Sharif ARM, Aris I, Janius R, Kamaruddin R. Design and development of a photovoltaic power system for tropical greenhouse cooling. Am J Appl Sci 2007;4(6):386–9.
[8] Juang P, Kacira M. System dynamics of a photovoltaic integrated greenhouse. Acta Hort 2014;1037:107–12.
[9] Rocamora MC, Tripanagnostopoulos Y. Aspects of PV/T solar system application for ventilation needs in greenhouses. Acta Hort 2006;719:239–46.
[10] Yano A, Tsuchiya K, Nishi K, Moriyama T, Ide O. Development of a greenhouse side-ventilation controller drive by photovoltaic energy. Biosyst Eng 2007;96(4):633–41. http://dx.doi.org/10.1016/j.biosystemseng.2006.12.012.
[11] Carlini M, Honorati T, Castellucci S. Photovoltaic greenhouses: comparison of optical and thermal behavior for energy savings. Math Probl Eng 2012:10. http://dx.doi.org/10.1155/2012/74376 743764.
[12] Dupraz C, Marrou H, Talbot G, Dufour L, Nogier A, Ferard Y. Combining solar photovoltaic panels and food crops for optimising land use: towards new agrivoltaic schemes. Renew Energy 2011;36(10):2725–32. http://dx.doi.org/10.1016/j.renene.2011.03.005.
[13] Castellano S. Photovoltaic greenhouses: evaluation of shading effect and its influence on agricultural performances. J Agric Engine 2014;XLV(433):168–74. http://dx.doi.org/10.4081/jae.2014.43.
[14] Cockshull KE, Graves CJ, Cave CRJ. The influence of shading on yield of glasshouse tomatoes. J Hortic Sci 1992;67(1):11–24.
[15] Heuvelink E. Growth, development and yield of a tomato crop: periodic destructive measurements in a greenhouse. Sci Hortic 1995;61:77–99. http://dx.doi.org/10.1016/0304-4238(94)00729-Y.
[16] Kläring H-P, Krumbein A. The effect of constraining the intensity of solar radiation on the photosynthesis, growth, yield and product quality of tomato. J Agro Crop Sci 2013;199:351–9. http://dx.doi.org/10.1111/jac.12018.
[17] Marcelis LFM, Broekhuijsen AGM, Meinen E, Nijs EMFM, Raaphorst MGM. Quantification of the growth response to light quantity of greenhouse grown crops. Acta Hortic 2006;711:97–104.
[18] Cossu M, Murgia L, Caria M, Pazzona A. Economic feasibility study of semitransparent photovoltaic technology integrated on greenhouse covering structures. In: Proceedings of the International Conference Ragusa SHWA, Work Safety and Risk Prevention in Agro-food and Forest Systems. Ragusa Ibla Campus. Ragusa, Italy; 2010. p. 648–55.
[19] Pérez-Alonso J, Pérez-García M, Pasamontes-Romera M, Callejón-Ferre AJ. Performance analysis and neural modelling of a greenhouse integrated photovoltaic system. Renew Sustain Energy Rev 2012;16:4675–85. http://dx.doi.org/10.1016/j.rser.2012.04.002.
[20] Yano A, Kadowaki M, Furue A, Tamaki N, Tanaka T, Hiraki E, et al. Shading and electrical features of a photovoltaic array mounted inside the roof of an east-west oriented greenhouse. Biosyst Eng 2010;106:367–77. http://dx.doi.org/10.1016/j.biosystemseng.2010.04.007.
[21] Ureña-Sánchez R, Callejón-Ferre ÁJ, Pérez-Alonso J, Carreño-Ortega Á. Greenhouse tomato production with electricity generation by roof-mounted flexible solar panels. Sci Agric 2012;69(4):233–9. http://dx.doi.org/10.1590/S0103-90162012000400001.
[22] Kadowaki M, Yano A, Ishizu F, Tanaka T, Noda S. Effects of greenhouse photovoltaic array shading on Welsh onion growth. Biosyst Eng 2012;111(3):290–7. http://dx.doi.org/10.1016/j.biosystemseng.2011.12.006.
[23] Minuto G, Bruzzone C, Tinivella F, Delfino G, Minuto A. Fotovoltaico sui tetti delle serre per produrre anche energia. Suppl L'Inform Agrario 2009;65(10):16–9.
[24] Cossu M, Murgia L, Ledda L, Deligios PA, Sirigu A, Chessa F, et al. Solar radiation distribution inside a greenhouse with south-oriented photovoltaic roofs and effects on crop productivity. Appl Energy 2014;133:89–100. http://dx.doi.org/10.1016/j.apenergy.2014.07.070.
[25] Chae YT, Kim J, Park H, Shin B. Building energy performance evaluation of building integrated photovoltaic (BIPV) window with semi-transparent solar cells. Appl Energy 2014;129:217–27. http://dx.doi.org/10.1016/j.apenergy.2014.04.106.
[26] Li DHW, Lam TNT, Chan WWH, Mak AHL. Energy and cost analysis of semi-transparent photovoltaic in office buildings. Appl Energy 2009;86:722–9. http://dx.doi.org/10.1016/j.apenergy.2008.08.009.
[27] Wong PW, Shimoda Y, Nonaka M, Inoue M, Mizuno M. Semi-transparent PV: thermal performance, power generation, daylight modelling and energy saving potential in a residential application. Renew Energy 2008;33:1024–36. http://dx.doi.org/10.1016/j.renene.2007.06.016.
[28] Marucci A, Monarca D, Cecchini M, Colantoni A, Manzo A, Cappuccini A. The semitransparent photovoltaic films for Mediterranean greenhouse: a new sustainable technology. Math Probl Eng 2012:14. http://dx.doi.org/10.1155/2012/45193 451934.
[29] Minuto G, Tinivella F, Bruzzone C, Minuto A. Con il fotovoltaico sul tetto la serra raddoppia la sua utilità. Suppl L'Inform Agrario 2011;38:2–6.
[30] Tani A, Shiina S, Nakashima K, Hayashi M. Improvement in lettuce growth by light diffusion under solar panels. J Agric Meteor 2014;70(3):139–49. http://dx.doi.org/10.2480/agrmet.D-14-00005.
[31] Yano A, Onoe M, Nakata Y. Prototype semi-transparent photovoltaic modules for greenhouse roof applications. Biosyst Eng 2014;122:62–73. http://dx.doi.org/10.1016/j.biosystemseng.2014.04.003.
[32] Papadopoulos AP, Pararajasingham S. The influence of plant spacing on light interception and use in greenhouse tomato (*Lycopersicon esculentum* Mill.): a review. Scientia. Horticulture 1997;69:1–29.
[33] Verheul MJ. Effects of plant density, leaf removal and light intensity on tomato quality and yield. Acta Hort 2012;956:365–72.
[34] Biancardo M, Taira K, Kogo N, Kikuchi H, Kumagai N, Kuratani N, et al. Characterization of microspherical semi-transparent solar cells and modules. Sol Energy 2007;81:711–6. http://dx.doi.org/10.1016/j.solener.2006.10.00.
[35] Taira K, Nakata J. Silicon cells: catching rays. Nature Photon 2010;4:602–3. http://dx.doi.org/10.1038/nphoton.2010.193.
[36] Markvart T. Solar electricity. 2nd ed. Chichester: John Wiley & Sons; 2000.
[37] Yano A, Furue A, Kadowaki M, Tanaka T, Hiraki E, Miyamoto M, et al. Electrical energy generated by photovoltaic modules mounted inside the roof of a north-south oriented greenhouse. Biosyst Eng 2009;103(2):228–38. http://dx.doi.org/10.1016/j.biosystemseng.2009.02.020.
[38] Photovoltaic Geographical Information System (PVGIS). European Commission. <http://re.jrc.ec.europa.eu/pvgis>.
[39] Kymakis E, Kalykakis S, Papazoglou TM. Performance analysis of a grid connected photovoltaic park on the island of Crete. Energy Convers Manage 2009;50(3):433–8. http://dx.doi.org/10.1016/j.enconman.2008.12.009.